Journal of Power Sources 353 (2017) 277–286

Contents lists available at ScienceDirect

Journal of Power Sources

journal homepage: www.elsevier.com/locate/jpowsour

Application of Buckingham π theorem for scaling-up oriented fast modelling of Proton Exchange Membrane Fuel Cell impedance

Luigi Russo, Marco Sorrentino*, Pierpaolo Polverino, Cesare Pianese

Department of Industrial Engineering, University of Salerno, Via Giovanni Paolo II, 132, 84084 Fisciano, SA, Italy

HIGHLIGHTS

- A methodology to reproduce PEMFC impedance is proposed.
- Non-dimensional parameters are defined by exploiting the Buckingham's π theorem.
- Good accuracy in PEMFC impedance prediction is proved.
- The possibility to use this methodology with scaling-up purposes is demonstrated.

ARTICLE INFO

Article history:
Received 17 November 2016
Received in revised form
23 March 2017
Accepted 24 March 2017

Keywords:
Electrochemical impedance spectroscopy
Proton exchange membrane fuel cell
Impedance modelling
Dimensional analysis
Scaling-up

ABSTRACT

This work focuses on the development of a fast PEMFC impedance model, built starting from both physical and geometrical variables. Buckingham's π theorem is proposed to define non-dimensional parameters that allow suitably describing the relationships linking the physical variables involved in the process under-study to the fundamental dimensions. This approach is a useful solution for those problems, whose first principles-based models are not known, difficult to build or computationally unfeasible. The key contributions of the proposed similarity theory-based modelling approach are presented and discussed. The major advantage resides in its straightforward online applicability, thanks to very low computational burden, while preserving good level of accuracy. This makes the model suitable for several purposes, such as design, control, diagnostics, state of health monitoring and prognostics. Experimental data, collected in different operating conditions, have been analysed to demonstrate the capability of the model to reproduce PEMFC impedance at different loads and temperatures. This results in a reduction of the experimental effort for the FCS lab characterization. Moreover, it is highlighted the possibility to use the model with scaling-up purposes to reproduce the full stack impedance from single-cell one, thus supporting FC design and development from lab-to commercial system-scale.

1. Introduction

Among the environmentally friendly energy conversion technologies, one of the most suitable solutions to cope with pollutant emissions and global warming issues are fuel cells, which have attracted the interest of many researchers in the last decades. In particular, the Proton Exchange Membrane Fuel Cell (PEMFC) has proved to be the most suitable for applications between 0.1 and 1000 kW [1]. The main advantages of PEMFCs are the high performance, modularity and potentially pollution-free operation. However, this technology has to meet specific technical requirements to become commercially competitive. US Department of Energy (DOE) and European Institutions have set clear technical targets to be achieved by PEMFC systems with costs and lifetime being the main issues; for stationary and automotive applications 40.000 h and 6000 h of operations are required, respectively ([2,3]).

In order to enhance FCS reliability and lifetime, control and diagnostics must be improved thanks to advanced monitoring algorithms, which must be fast enough to operate on-field to obtain effective advantages. Advanced techniques are required to analyze performance losses caused by degradation mechanisms and the impact of the current operating conditions.

The most effective methods used to characterize the performance of a fuel cell are electrochemical techniques, such as Electrochemical Impedance Spectroscopy (EIS), polarization curves,

* Corresponding author.
E-mail address: msorrentino@unisa.it (M. Sorrentino).

http://dx.doi.org/10.1016/j.jpowsour.2017.03.116
0378-7753/© 2017 Published by Elsevier B.V.

cyclic voltammetry, AC impedance and current interruption techniques [4]. Among these techniques, EIS is the most suitable to recognize the individual contributions related to voltage drops caused by membrane, charge transfer and mass transfer resistances, both for single cells and overall stack [5]. The EIS technique is used to measure the frequency dependence of the impedance of a fuel cell by applying a small sinusoidal AC voltage (or current) as a perturbation signal to the fuel cell and measuring the current (or voltage) response. This is done at different frequencies for each load to obtain the overall system impedance, often plotted as Nyquist diagram [6]. The applications of EIS in PEMFC studies allows providing electrochemical information about the FCS, which can then help in fuel cell structure optimization and selection of the most appropriate operating conditions. The EIS appears to be the most suitable method for fuel cells on-field monitoring and control, thanks to its peculiar characteristics [7]. Indeed, the main advantage of using EIS resides in the possibility to recognize the contributions of each physical phenomenon (i.e. ohmic losses, charge-transfer and diffusion limitations) to the full impedance thanks to the Equivalent Circuit Modelling (ECM), which consists in modelling the cells using equivalent circuits. Therefore, each contribution can be identified since each circuital parameter represents a physical phenomenon occurring inside the fuel cell [8]. Moreover, the analysis of the ECM parameters may be useful to distinguish between normal and faulty operations [9]. The use of Fractional Order Modelling (FOM), instead, has been proposed as a very suitable approach to model transients and time depending phenomena [10].

Many authors have demonstrated the capability to detect faults using the EIS by recording impedance spectra during fuel cell operation and analysing these data using the ECM approach with diagnostic purposes ([11,12]). The paper of Narjis et al. [13] provides the main references for the development of Fault Detection and Isolation (FDI) based on EIS [7]. Also the use of more physical-based modelling representation of fuel cell impedance has been thoroughly accounted for in the literature. For example, Kulikovsky proposed the analytical model of a the impedance of a PEMFC cathode catalyst layer under poor oxygen transport ([14,15]) and at Open Circuit Voltage in addition to the Gas Diffusion Layer impedance [16]. The work of Cruz-Manzo et al. [17] describes the PEMFC impedance spectra subject to Pt oxidation and H_2 peroxide formation at cathode side, also with the combined use of physical and circuit modelling. On the same line, Cruz-Manzo et al. [17] and Niya et al. [18] developed an impedance model combining physical and ECM approaches, particularly aiming at describing a PEMFC impedance at different operating conditions, varying current densities, temperature and humidity levels. Physics-based PEMFC impedance models were also developed by Setzler and Fuller [19], with the implementation of an oxide growth oxygen reduction reaction kinetic model, and Chevalier et al. [20,21], aiming at PEMFC state-of-health and degradation analysis. The analysis of the cells Output Voltage Signal with Discrete Wavelet Transform (DWT) and Continuous Wavelet Transform (CWT) has been also proposed for fuel cells FDI in the recent literature ([22,23]).

The EIS methodology, however, has its drawbacks. The traditional EIS equipment is costly and cumbersome and requires several minutes to record a single impedance spectrum. Moreover, the diagnosis can be performed once some metrics are derived through EIS signal treatment. This is not a simple task because, in many cases, different operating conditions could lead to the same impedance spectrum; thus, a deep analysis based on analyst experience is necessary. On the other hand, for on-field (i.e. unattended) operations suitable algorithms, such as those based on the ECM [24] or on FOM approaches [10], can be built to process the EIS to derive useful metrics for monitoring and diagnostic applications.

The scientific contribution of the present work is the development of a fast model capable of simulating PEMFC impedance spectra. The model is based on non-dimensional parameters defined by exploiting the Buckingham's π Theorem, which is a key method in the similarity theory field. Particularly, it allows suitably describing the relationships linking the physical variables involved in the process under-study to the fundamental dimensions [25]. The definition of non-dimensional parameters allows reproducing the impedance of different types of system operating at different conditions, thanks to the high generalizability of the model. Therefore, the development of such a model does not require large experimental data; moreover, its simple algorithms need few coding operations, low experimental efforts and are computationally efficient (i.e. fast), allowing easily implementation on low cost hardware as well. This method may be then used for several purposes either for design purposes, by exploiting its scaling-up features, or on-system implementation for on-field use such as on-line applications (e.g. monitoring, diagnostics, control, state of health management and prognostics). The authors have already discussed the significant capabilities associated to the proper exploitation of similarity theory for optimal design and management of innovative energy systems, including fuel cell vehicles ([26–28]). The scaling-up features of the presented method allow using either single-cell or short stack arrangements to characterize the electrochemistry, so as to simulate the behaviour of the full stack. During prototyping phases, this may help in reducing hardware costs (for both test bench and cell materials), as well as consumables. Moreover, it is also beneficial in those problems where the occurrence of degradation and faults should be tested under different operating conditions, i.e., when non-optimal control variables are imposed. It is a matter of fact that to characterize FCS several experimental tests have to be performed under different loads. Moreover, to be able to identify occurring faults, tests in faulty operating conditions have to be performed too. These tests are very degradative and implies FCS fast end-of-life. Thanks to the proposed similarity theory-based modelling approach, the latter issues can be avoided by performing a unique EIS measurement at fixed operating conditions, thus obtaining the behaviour of the FCS under different operating conditions by re-characterizing the non-dimensional parameters.

The model developed following the Buckingham theory is mainly achieved through a data-driven approach, which links measured impedance data and physical models to shape the non-dimensional parameters required for the problem description and generalization.

In the following, the description of the overall model is firstly given, starting from the definition of the non-dimensional parameters towards the description of each involved variable. The design problem is formulated considering both physical and electric variables, which are representative of fuel cell impedance (as detailed in Section 2.1). Therefore, key features of both ECM-based and physics-based methods are accounted for. Nevertheless, it is worth observing that the characterization of these non-dimensional parameters requires the use of impedance data provided by experimental tests. The use of such data allows shaping the fuel cell impedance through the non-dimensional parameters by means of proper physical variables (e.g. temperature, current, water content, fuel utilization, etc.), whose values depend on the specific conditions that have to be simulated. Therefore, the novelty of this approach resides in its structure and development process, which could be considered as black-box if seen from a mathematical point of view (as could be any polynomial regression). However, as said, it gathers properties of both ECM-based and physical-based representations: the impedance layout is given by the measured data required for non-dimensional parameters evaluation (without requiring any ECM model), and the scaling-up process is fulfilled through physical reasoning (e.g. inference on fuel and/or water distribution or other significant parameters). According to these comments, the main advantage of using such an approach, with respect to ECM or physics-based methods, consists in the easy and quick impedance scalability, achieved through proper scalability factors (as for instance those used in other disciplines like fluid- and thermal-dynamics through Reynolds and Prandtl numbers), without requiring high computational processes or complex models. This gives further degree of freedom in the impedance representation, without requiring the definition of, e.g., a specific impedance or model shapes. Afterwards, the paper deals with the application of the methodology both to reproduce PEMFC impedance at different operating conditions and simulate PEMFC impedance from single-cell to full stack (i.e. scaling-up). This study is supported by the analysis of experimental data available in the literature ([29–31]) which were particularly deployed to assess model accuracy as well as the scaling-up potentialities of the proposed methodology. To authors knowledge, no previous contributions were given on the application of Buckingham theorem to PEMFC impedance shape reproduction.

2. PEMFC impedance model

The idea of developing a fast PEMFC impedance model arises since the most suitable method used in FCs diagnostics and control is based on EIS measurements. However, the current methodology, that involves the analysis of the measurements through circuital modelling, might be time consuming and would require further work for its on-line application within FDI algorithms [6]. On the other hand, the model proposed in this study has the advantage of being computationally efficient and easily generalizable, thanks to the exploitation of non-dimensional parameters obtained via a dimensional analysis of the involved physical quantities.

2.1. Dimensional analysis

The developed model uses non-dimensional parameters to reproduce the PEMFCs impedance. To define these parameters, the Buckingham's π theorem has been exploited ([25,32,33]). This approach has been previously used to address both engineering [34] and electrochemical [35] problems. The theorem states that if there is a physically meaningful equation involving a number n of physical variables, then the original equation can be rewritten in terms of a set of non-dimensional parameters π_0, π_2, …, π_{p-1} built from the original variables. Let be Q_0 a physical variable of interest that is a “dependent variable” in a known process. This means that once all the independent quantities are specified the value of Q_0 follows uniquely. The procedure to identify the non-dimensional parameters that can simplify and generalize the problem is the following [36]:

Step 1: Identify a complete set of independent quantities Q_1, Q_2, …, Q_n that allow determining the value of Q_0:

$$Q_0 = f(Q_1, Q_2, \ldots, Q_n) \tag{1}$$

Step 2: List the dimensions of the dependent and all the independent variables. Since the addressed problem is electrical, all the quantities are defined in terms of the four fundamental dimensions (i) mass $[M]$, (ii) length $[L]$, (iii) current $[I]$ and (iv) time $[T]$:

$$[Q_i] = L_i^l M_i^m T_i^\tau I_i^j \tag{2}$$

where the exponents l_i, m_i, τ_i and j_i are dimensionless numbers that follow from each quantity's definition and $i = 0, n$.

Step 3: Pick from the entire set of independent variables a “complete” and “dimensionally independent” subset and express the dimensions of the remaining variables, including the dependent variable Q_0, as a product of powers of this subset. A subset is “dimensionally independent” if none of the variables included has dimensions that can be expressed in terms of the dimensions of the remaining variables included. It is “complete” if the dimensions of all the remaining quantities outside the subset can be expressed in terms of the dimensions of the subset. The determination of this subset is driven by heuristic or trial and error approaches. It involves k variables, with $k \le v$, where v is the number of involved fundamental dimensions.
Step 4: Define the non-dimensional parameters. The number of non-dimensional parameters is evaluable as:

$$p = n - k \tag{3}$$

Afterword, the non-dimensional parameters are obtained by dividing the variables not included in the previously defined subset with the product of the variables included in the subset:

$$\pi_i = \frac{[Q_i]}{[Q_1]^{N_{(i)1}} \cdot [Q_2]^{N_{(i)2}} \ldots \cdot [Q_k]^{N_{(i)k}}} \tag{4}$$

where $N_{(i)1}$, $N_{(i)2}$, …, $N_{(i)k}$ are the powers that zero the dimensions and $i = 0, (p-1)$. The result is a simplification of the overall problem, mainly due the reduction of the number of involved quantities. Indeed, the problem can be rewritten as:

$$\pi_0 = f(\pi_1, \pi_2, \ldots, \pi_{p-1}) \tag{5}$$

where π_0 is the non-dimensional parameter defined from the dependent variable Q_0.

The PEMFC impedance can be defined as a function of specific variables, either physical [37] or electrical [38], used to describe the electrochemical phenomena that take place inside the cells. Therefore, the PEMFCs impedance is here defined as a function of both electrical and electrochemical variables:

$$Z = f(R_{eq}, \ C, \ \omega, \ I, \ ECSA) \tag{6}$$

where R_{eq} represents the equivalent electric resistance, C the electric capacitance, ω the frequency, I the electric load and $ECSA$ the electrochemical surface area. The equivalent electric resistance describes the linear losses (e.g. membrane resistance and charge-transfer resistance) while the electric capacitance shapes the non-linear ones (e.g. energy accumulation over the electrodes). Therefore, after Eq. (6), the number n of physical variables involved in the problem is six. According to the π theorem procedure, the dimensions of these variables are expressed in terms of the v fundamental dimensions: (i) mass $[M]$, (ii) length $[L]$, (iii) current $[I]$ and (iv) time $[T]$, as described in Eq. (7).

$$\begin{cases} [Z] = \left[M^1L^2I^{-2}T^{-3}\right] \\ \left[R_{eq}\right] = \left[M^1L^2I^{-2}T^{-3}\right] \\ [C] = \left[M^{-1}L^{-2}I^2T^4\right] \\ [\omega] = \left[M^0L^0I^0T^{-1}\right] \\ [I] = \left[M^0L^0I^1T^0\right] \\ [ECSA] = \left[M^0L^2I^0T^0\right] \end{cases} \tag{7}$$

Following the procedure described in *Step 3*, the complete and dimensionally independent subset is defined: it includes the variables R_{eq}, ω, I and $ECSA$. Thus, the number of non-dimensional definable parameters to describe the overall problem, according to Eq. (3), is two ($n = 6$ and $k = \nu = 4$). The first is that one obtained from the dependent variable Z, the second one is obtained from the independent variable C. Following the aforementioned procedure:

$$\pi_0 = \frac{Z}{R_{eq}^{N_{01}}\omega^{N_{02}}I^{N_{03}}ECSA^{N_{04}}} = \frac{\left[M^1L^2I^{-2}T^{-3}\right]}{\left[M^1L^2I^{-2}T^{-3}\right]^{N_{01}}\left[T^{-1}\right]^{N_{02}}\left[I^1\right]^{N_{03}}\left[L^2\right]^{N_{04}}} = \left[M^0L^0I^0T^0\right] \tag{8}$$

As long as the objective is to obtain non-dimensional parameters, the following system has to be solved to obtain the powers N_i:

$$\begin{cases} 1 - N_{01} = 0 \\ 2 - 2N_{01} - 2N_{04} = 0 \\ -2 + 2N_{01} - N_{03} = 0 \\ -3 + 3N_{01} + N_{02} = 0 \end{cases} \Rightarrow \begin{cases} N_{01} = 1 \\ N_{04} = 0 \\ N_{03} = 0 \\ N_{02} = 0 \end{cases} \tag{9}$$

So, the unique value different from zero is N_{01}. Thus, the first non-dimensional parameter is:

$$\pi_0 = Z/R_{eq} \tag{10}$$

Following the same procedure for the variable *C*:

$$\pi_1 = \frac{C}{R_{eq}^{N_{11}}\omega^{N_{12}}I^{N_{13}}ECSA^{N_{14}}} = \frac{\left[M^{-1}L^{-2}I^2T^4\right]}{\left[M^1L^2I^{-2}T^{-3}\right]^{N_{11}}\left[T^{-1}\right]^{N_{12}}\left[I^1\right]^{N_{13}}\left[L^2\right]^{N_{14}}} = \left[M^0L^0I^0T^0\right] \tag{11}$$

In this case, the system to be solved is:

$$\begin{cases} -1 - N_{11} = 0 \\ -2 - 2N_{11} - 2N_{14} = 0 \\ 4 + 3N_{11} + N_{12} = 0 \\ 2 + N_{11} - N_{13} = 0 \end{cases} \Rightarrow \begin{cases} N_{11} = -1 \\ N_{14} = 0 \\ N_{12} = -1 \\ N_{13} = 0 \end{cases} \tag{12}$$

leading to the second parameter:

$$\pi_1 = CR_{eq}\omega \tag{13}$$

The first parameter is the normalization of the total impedance over the equivalent resistance, while the second one is a time dependent group. The two non-dimensional parameters obtained are referred, from now on, as G and κ, respectively. The outcomes of the above-described dimensional analysis underline that two non-dimensional parameters are necessary overall to define the impedance. Since the total impedance involves real and imaginary parts, it is possible to distinguish between real and imaginary parts of G, defined as real and imaginary parts of the total impedance normalized over the equivalent resistance, as shown in Eq. (14):

$$\begin{cases} G = Z/R_{eq} \Rightarrow \begin{cases} G_r = \mathrm{Re}(Z)/R_{eq} \\ G_i = \mathrm{Im}(Z)/R_{eq} \end{cases} \\ \kappa = CR_{eq}\omega \end{cases} \tag{14}$$

Thanks to this simplification, to reproduce impedance spectra in the Nyquist diagram at different operating conditions or for different system sizes, only the parameters G_r and G_i are needed. These parameters can be identified from EIS experimental data. Indeed, the variables $\mathrm{Re}(Z)$ and $\mathrm{Im}(Z)$ are known data coming from EIS measurements (i.e. real and imaginary part of the cell impedance and vector of the scanned frequencies, respectively). The equivalent resistance, indeed, is defined by exploiting suitable models, as described in the next section.

2.2. Variables modelling

Thanks to the dimensional analysis and the application of the Buckingham's Theorem, the non-dimensional parameters capable to simplify and generalize the problem have been defined in Eq. (14). Fig. 1 shows the effective steps, to be undertaken to fruitfully exploit the proposed approach for PEMFC impedance modelling, as well as for scaling purposes.

In the *identification* phase, $\mathrm{Re}(Z)$ and $\mathrm{Im}(Z)$ (i.e. real and imaginary parts of the impedance) are derived from an existing EIS data set and, thanks to the physical and empirical models detailed below, within this section, R_{eq} is computed, so that the non-dimensional parameters G_r and G_i can be successfully identified (see Eq. (14)).

Then, to obtain impedance behaviour in different operating conditions or for different system size, in the *scaling* phase R_{eq} has to be recomputed in accordance with the conditions to be predicted (e.g. if the objective is to predict impedance behaviour in different load conditions, the value of the load I must be changed, whereas if the objective is to scale the impedance to higher power systems, geometrical parameters have to be adjusted, etc.). The scaling procedure will result in a new value of the total resistance R^*_{eq}, as well as of the real and imaginary parts to be predicted, i.e. $\mathrm{Re}^*(Z)$ and $\mathrm{Im}^*(Z)$, as shown in Eq. (15):

$$\begin{cases} \mathrm{Re}^*(Z) = G_r\, R^*_{eq} \\ \mathrm{Im}^*(Z) = G_i\, R^*_{eq} \end{cases} \tag{15}$$

The equivalent resistance R_{eq} is the sum of ohmic (R_m) and charge-transfer (R_{ct}) losses. This results from having assumed the mass transfer contribution negligible because, at this moment, the overall model mainly aims at reproducing PEMFC impedance spectra in normal operating conditions, whereas, as it is well-known, mass transfer losses are usually associated to abnormal operating conditions (e.g. if the stack were operated at loads higher than what is recommended by the manufacturer, an accentuated mass transfer arc would occur in the impedance spectrum). However, for future prospects (i.e. PEMFC diagnosis and prognosis), it has been considered by the authors the addition of the mass transfer losses related variables (such as H_2 inlet pressure), so as to make the overall model robust also in case of abnormal operating conditions.

Thus, the equivalent resistance is:

$$R_{eq} = R_m + R_{ct} \tag{16}$$

The ohmic resistance can be computed using the model proposed by Springer [39]:

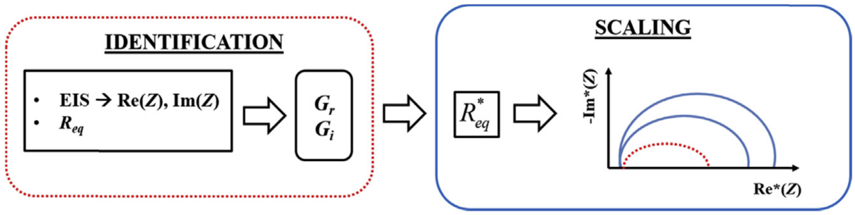

Fig. 1. Scheme of the proposed scaling-up methodology.

$$R_m^{Springer} = \frac{l_m}{\sigma_m} \cdot \frac{1}{A} \tag{17}$$

where l_m is the membrane thickness, A is the electroactive area, and σ_m is the membrane conductivity, expressed as:

$$\sigma_{\mathrm{m}} = \exp\left[1268\left(\frac{1}{303} - \frac{1}{T_S}\right)\right] \cdot \sigma_{30} \tag{18}$$

From Eq. (18), it is possible to note that the conductivity is expressed as a function of the mean temperature of the stack (T_S) and the parameter σ_{30}, which is the conductivity at 30 °C defined as function of the membrane humidification [39]:

$$\sigma_{30} = 0.005139\,\lambda_m - 0.00326 \tag{19}$$

Alternatively, the membrane resistance can be expressed by exploiting the model of Mann [40]:

$$R_m^{Mann} = 181.6 \cdot \left(\frac{1 + 0.03 \cdot \left(\frac{I}{A}\right) + 0.062 \cdot \left(\frac{T_S}{303}\right)^2 \cdot \left(\frac{I}{A}\right)^{2.5}}{\lambda_m - 0.634 - 3 \cdot \left(\frac{I}{A}\right) \exp\left(1 - \frac{303}{T_S}\right)} \right) \cdot K_m \tag{20}$$

In this case, the membrane resistance is expressed as a function of the current density (I/A), the cell temperature expressed in Kelvin degrees (T_S), the membrane humidification level λ_m and the parameter K_m, related to the membrane thickness. The membrane humidity level λ_m is function of the relative humidity (RH), which represents a clear indicator of the amount of water that wets the membrane. It is defined as the ratio of the partial pressure of the water vapour to the equilibrium vapour pressure:

$$RH = P_w / P_{sat} \tag{21}$$

Considering Nafion® 117, as long as this type of membrane has been largely adopted in PEMFC applications (and thus in the literature a large amount of studies is available that allows obtaining the relationship between RH and λ_{m}, useful in modelling ohmic losses ([39–41])), membrane humidification reaches the value $\lambda_m = 14$ at a relative humidity of 1. At this condition, the ohmic resistance assumes the smallest possible value as demonstrated so far by Springer [39], and confirmed by Kawamura [41], who has investigated further operating conditions. For values of $\lambda_m < 14$ (membrane drying) the ohmic resistance increases; for values of $\lambda_m > 14$ (membrane flooding), instead, the ohmic resistance remains the same, but the high presence of water at both sides could cause reactants starvation, as well as an increase in diffusive transport.

The data collected by Kawamura [41] have been used to obtain a polynomial function that correlates the membrane humidification and RH as follows:

$$\lambda_m = 35.9 \cdot RH^3 - 39.6 \cdot RH^2 + 17.7 \cdot RH + 0.0441 \tag{22}$$

It is worth clarifying that, for different technologies, it is possible reproducing the ohmic losses by changing membrane conductivity in the variables models, in accordance with the material of the membranes.

The relative humidity value has been fixed at the stack middle-cell and it has been considered equal to 1 for the closed-cathode stacks and 0.6 for the open-cathode ones, because it is well known that this type of stacks works in dryer conditions as it is characterized by a very high airflow that dries the membrane on the cathode side moving the water outside faster than it is created. Moreover, it has been hypothesized that RH has linear behaviour increasing/decreasing by 2% per cell going toward air and fuel inlet, respectively. This is an empirical hypothesis consequence of the well-known water distribution along the stack, from the H_2 inlet to the Air/O_2 one. Indeed, the cells closer to the Air/O_2 inlet, show a higher water content compared to the cells closer to the H_2 inlet. Also for the Fuel Utilization (FU), a linear distribution has been adopted: FU increases linearly from the 1st cell till the last one (from 0.1 to 1) (Fig. 2). The linear behaviours have been adopted for simplicity and to make the algorithm (that has real-time applications purposes) faster; the overall precision, shown in the following results section, is the proof of concept that this hypothesis is not so far from the real behaviour of the water distribution inside the stack.

The charge-transfer resistance (R_{ct}) is expressed through a regression obtained by exploiting experimental data collected in different operating conditions. In particular, R_{ct} is expressed as a function of the current, temperature, electrodes area and number of cells (Eq. (23)). The regression is obtained from data collected in the framework of the European Project D-CODE [29]. In particular, the ECM algorithm proposed by Petrone in his PhD Thesis [42] has been exploited to obtain the value of the charge transfer resistance at different operating conditions; such values were then regressed as a function of stack mean temperature expressed in Celsius degrees (T_S) and stack current load I, thus resulting in the following correlation:

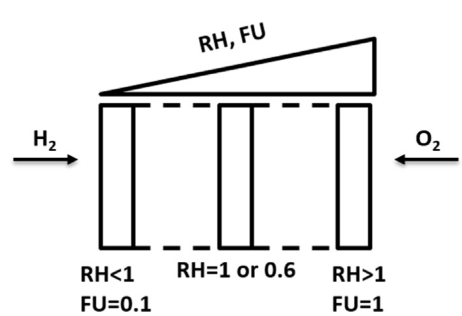

Fig. 2. Hypothesis adopted for modelling RH and FU distribution along the stack.

$$R_{ct} = 13.2 + 15.9\frac{1}{I} + 15.4\frac{1}{I^2} + 0.359\,T_S + 0.00272\,T_S^2 \qquad (23)$$

It is worth remarking that the procedure implies the identification of the non-dimensional parameters behaviour on a set of EIS experimental data. Once the polynomials that define the real and imaginary parts of G as function of κ are identified, these parameters have to be re-characterized through the aforementioned physical and mathematical models to obtain impedance spectra for different system size (i.e. scaling-up) or at different operating conditions (e.g. higher current loads).

As mentioned in the previous sections, the proposed approach requires the use of measured impedance data to characterize the non-dimensional parameters of the Buckingham theorem. The shape of the data used in this task reflects part of the scaled impedance shape: if the measured impedance shows a depressed half circle, the scaled up ones may show it as well. However, the scaling up process also plays an important role through the introduction of proper values of the accounted physical parameters. The proposed model involves both electric and physical variables and represents an extension of the ECM approach. Differently from a simple ECM that uses only electric parameters, the proposed approach allows linking the phenomena that take place inside the cells to the correspondent physical variables (e.g. *RH*, *FU*, electroactive area, membrane conductivity, etc.). It is precisely thanks to the physical formulation of the involved variables (i.e. modelling R_m with Springer or Mann laws, modelling R_{ct} as a function of current and temperature, etc.) that it results possible to reproduce the impedance behaviour of the cells in different operating conditions and for different systems size. Indeed, the suitable definition of fuel or water content distribution (as introduced in the following) allows catching impedance deformation due to, e.g. faults or degradation processes. The present algorithm cannot thoroughly represent all the possible shapes a fuel cell impedance spectrum may show.

Indeed, thanks to this approach, that exploits the advantages of the similarity theory combined with physical models of the variables, it is possible to reproduce accurately the PEMFC impedance. In the next section, the capability of the model to reproduce PEMFC impedance both in different operating conditions and for different stack sizes is shown.

3. Results

The proposed model allows obtaining the PEMFC impedance in different operating conditions and could be used with different purposes. In this section, the capability to reproduce the impedance starting from a unique set of experimental data is shown. The last section of the chapter is dedicated to the scaling-up. The scaling-up has, by definition, the objective to migrate a process from the lab-scale to the pilot plant-scale or commercial scale [44]. During the design phase, it is common use performing degradative tests on entire FCS to characterize these systems and their behaviour operating in faulty conditions. These tests are very expensive as they imply fast end-of-life of the systems. It is possible to avoid this problem by testing single-cells to get their behaviour under faulty operating conditions and, then, scaling-up the results to the whole fuel cell systems.

3.1. PEMFC impedance at different current loads

To characterize FCS, many tests in different operating conditions should be performed. To reduce the number of tests and, thus, time and cost efforts, the proposed methodology can be adopted. In this way, only one test at a fixed current load is needed to fully characterize the FCS, provided that the extension of the black-box model, here proposed for charge transfer resistance estimation (see Eq. (23)), is proven valid. To validate the model capability to predict PEMFC impedance spectra in different operating conditions, the experimental data collected in the framework of the D-CODE European project [29] and those one available from the paper of Asghari [30] have been used. In Table 1 are collected the main characteristics of the stacks tested in the framework of these works. It is worth remembering that the PEMFC impedance spectrum, when represented on the Nyquist diagram, is characterized by one arc related to the cathodic losses. Indeed, the losses related to anode and mass transport limitations are negligible in normal operating conditions. Thus, as the current load increases, the PEMFC impedance arc shrinks [1].

In Figs. 3 and 4 the results in reproducing the impedance spectra at different currents for the two datasets are shown. The non-dimensional parameters (Eq. (14)) have been identified on the data acquired at 5 A and 20 A for D-CODE and Asghari, respectively (see Table 1). These have been than scaled, following the procedure described in the previous section (Fig. 1), to obtain the spectra at 10, 25 and 40 Amps for D-CODE (Fig. 3), and 40 and 60 Amps for Asghari (Fig. 4). The experimental data are depicted with empty markers, whereas model results are depicted with filled markers; the lines colours are similar for equal loads. The impedance has been normalized multiplying by the area and dividing by the number of cells. At first glance, a good accordance emerges between the experimental data and the model predictions.

Focusing on Fig. 3, it is possible to note that the precision of the model predictions decreases as the load increases. This could be due to the fact that the temperature of the stack changes with the current, while in the model it is fixed at the value assumed at 5 A, because in the real application of the proposed methodology the temperature at higher loads may be unknown. Indeed, for the data of Asghari (Fig. 4), which have been acquired at fixed temperature (i.e. 55 °C), the precision is higher for all the loads. Anyway, the precision is high for all the analysed cases and it is comparable to that one obtainable by using equivalent circuit modelling [7]. This confirms the possibility to perform less laboratory tests to fully characterize stacks behaviour under different loads conditions, mainly thanks to the good accuracy guaranteed by the here proposed similarity theory-based model to reproduce PEMFC impedance shape. It is finally worth remarking that the charge transfer resistance model (i.e. Eq. (23)) was identified on the D-CODE data set [29]. Afterwards, such a sub-model was directly extended, with minor adaptation, to Ashgari data set [30], thus fully demonstrating the genericity and the potential technology independent deployment of the proposed procedure.

3.2. Scaling-up of PEMFC impedance: from single-cell to full stack

The scaling-up of fuel cells is usually performed after the single-cell has successfully met its targets of durability and reliability,

Table 1
Specifications of tested stacks. Further details can be retrieved from Refs. [29,30].

	Nominal Power	Number of cells	Electroactive Area	Type of Membrane	Operating Temperature	*RH*
D-CODE stack	2 kW	56	157 cm^2	Nafion 117	30–70 °C	0.6–0.9
Asghari stack	480 W	3	225 cm^2	Nafion 112	55 °C (kept constant)	0.95 (kept constant)

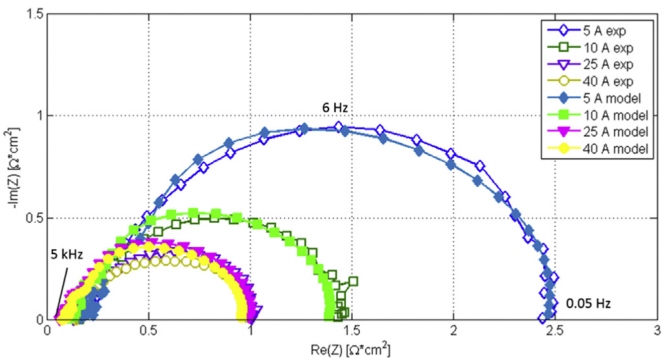

Fig. 3. Results in PEMFC impedance prediction at different operating currents (D-CODE data [29]). The experimental data are depicted with empty markers, whereas model results are depicted with filled markers.

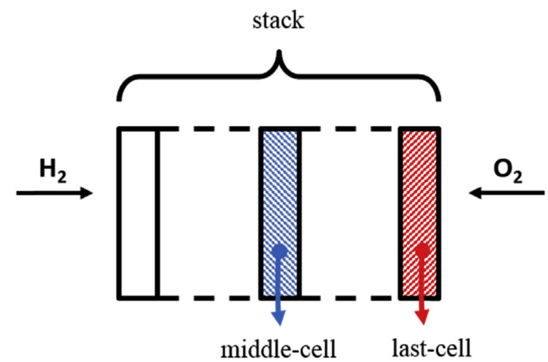

Fig. 5. Schematic visualization of the cells, which were selected for identifying non dimensional parameters in the two analyses presented in Sections 3.2.1. and 3.2.2.

including all the components in the cell, such as membrane, GDL, CL, BP and electrodes. However, the performance of the stack or of the entire FCS are difficult to derive from the single-cell data. Wang ([43,44]) in his studies describes this issue and the necessity to compute and optimize the flows distribution thanks to flow field design that needs CFD analysis. Paliniswamy [45] have conducted similar studies with the objective to scale-up PEMFC with different flow fields from 25 to 70 cm^2. In the work of Bonnet [46], instead, a comparison between a 25 cm^2 single-cell, a 340 cm^2/5-cell pilot stack and 800 cm^2/90-cell stack is shown to define the best operating conditions, yielding the highest performance and the lowest degradation on the complete 80 kW FCS. Despite to sophisticated and time-consuming methodologies based on CFD analysis, the possibility to scale-up electrochemical systems by exploiting Similarity Theory thanks to the definition of non-dimensional parameters is discussed in the works of Rao [47] and Sulaymon & Abbar [48]. The data analysed to validate the scaling-up capability of the proposed method are those collected by Wasterlain [31]. These data include the impedance spectra of a 20 cell PEMFC stack (with electrodes area of 100 cm^2) recorded both for each cell and for the overall stack. According to the procedure described in the previous section (Fig. 1), from the treatment of the impedance data of a single-cell the non-dimensional parameters G and κ have been derived. Once the polynomials defining the real and imaginary parts of G as function of κ had been computed, these parameters have been re-characterized to obtain the overall impedance of the stack.

As it can be noted, the last-cell is characterized by higher diffusion losses. This can be due to the flow distributions in the stack. Indeed, the last cell is the closest to the air inlet and the fuel outlet: the accumulation of water in this zone is an obstacle to the hydrogen flow [31]. Fig. 5 provides an explanation of the two different analyses done by exploiting the data collected by Wasterlain et al. [31]. Particularly, the first analysis was carried-out by identifying the non-dimensional parameters on the stack middle-cell and then scaling R_{eq} to obtain the stack total impedance; the second analysis, instead, was performed by identifying the non-dimensional parameters on the stack last-cell and then scaling R_{eq} to obtain the stack total impedance.

3.2.1. From stack middle-cell to whole stack impedance

In Fig. 6 the comparison between the results obtained by exploiting the models of Springer (Eq. (16)) and Mann (Eq. (19)) for the membrane resistance are shown. To identify the non-dimensional parameters, the data related to the stack middle-cell have been considered. These data have been used to reproduce the stack impedance. From the comparison of the stack experimental data and the models predictions, a good accordance emerges. The comparison of the percentage errors of the models predictions, by using Mann and Springer models for the membrane resistance, with respect to the experimental data are shown in Table 2. Here, the percentage errors to predict R_m (that is the impedance arc 1st intercept on the real axis), R_{ct} (that is the 2nd intercept on the real axis) and the maximum value of the impedance imaginary part (absolute value) are shown. The resulting accuracy is similar and the use of one rather than the other is related to the scope of the analysis. If the objective is to migrate experimental data collected with a PEMFC made with Nafion 112 to a stack made with different materials, for instance, the model of Springer is useful because it involves the dependence by the membrane conductivity.

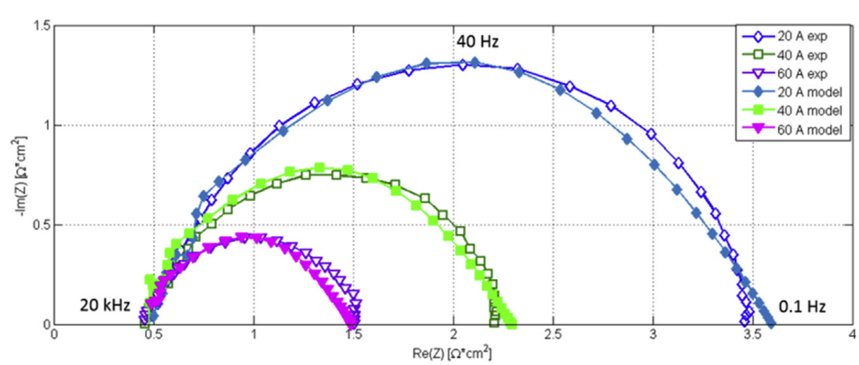

Fig. 4. Results in PEMFC impedance prediction at different operating currents (Asghari data [30]). The experimental data are depicted with empty markers, whereas model results are depicted with filled markers.

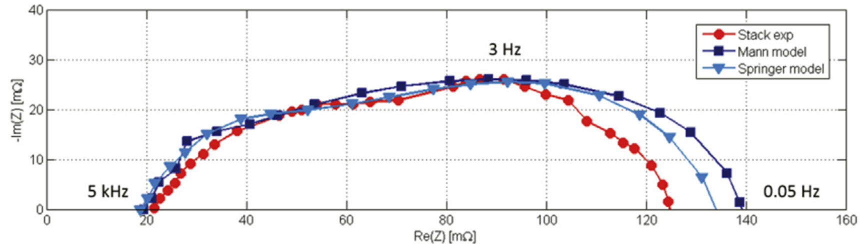

Fig. 6. Comparison of stack measured impedance (●) with the results yielded by the proposed methodology, particularly by using the models of Mann (■, see Eq. (20)) and Springer (▼, see Eq. (17)), respectively.

Table 2
Comparison of the percentage errors in PEMFC stack impedance prediction by using Mann and Springer models for the membrane resistance.

	Results using Mann model for R_m	Results using Springer model for R_m
R_m	6.6%	9.8%
R_{ct}	12%	7.5%
Max(Im(Z))	0.1%	2.4%

3.2.2. From stack last-cell to whole stack impedance

In Fig. 7, instead, the results obtained scaling the impedance of the stack last-cell are reported. The non-dimensional parameters have been identified by exploiting the EIS data related to the worst cell in terms of water content (in this case the closest to the air inlet, that results flooded). This choice has been done to validate the model capabilities and its robustness: indeed, the simple multiplication of the impedance of this cell by the number of cells (Single-cell*Ncell) does not allow obtaining good prediction of the overall stack impedance, while by using the proposed methodology, even if the non-dimensional parameters have been identified using the more flooded cell, the total stack impedance prediction (Scaling-up) is in good accordance with the value measured experimentally (Stack exp).

Here is also reported the spectrum obtainable with the simple multiplication of the single-cell impedance times the number of cells to highlight that it is not suitable this simple multiplication to obtain the full-stack impedance; in fact, this multiplication implies an overestimation of the stack total impedance, while the model allows obtaining a good prediction. Indeed, the results obtained for the full-stack impedance prediction have a precision comparable to equivalent circuit methods [7] with a mean percentage error, calculated by exploiting Eq. (24)–(25), of 10 and 20% to predict real and imaginary parts, respectively.

$$\frac{\sum\left(\left|\mathrm{Re}(Z)-\mathrm{Re}^*(Z)\right|\right)/\mathrm{Re}(Z)}{n_p}\cdot 100 \tag{24}$$

$$\frac{\sum\left(\left|\mathrm{Im}(Z)-\mathrm{Im}^*(Z)\right|\right)/\mathrm{Im}(Z)}{n_p}\cdot 100 \tag{25}$$

In Table 3 are collected the non-dimensional parameters G_r and G_i defined through the proposed approach for the different analyses shown in this section.

4. Conclusions

This work presents a methodology to reproduce PEMFC impedance shape thanks to non-dimensional parameters defined by exploiting the Buckingham's π Theorem, a key method in the similarity theory field. The procedure implies the identification of the non-dimensional parameters on a unique set of experimental data. After that, by re-characterizing these parameters, it is possible to reproduce PEMFC impedance in different operating conditions (e.g. current loads, operating temperatures, membrane humidification level, etc.) and for different system size (i.e. scaling-up). The capabilities of the method have been validated on data present in literature by comparing the model results and the experimental data. The precision of the model is comparable to that one obtainable using equivalent circuit modelling approach. Thanks to the proposed methodology, it could be possible to reproduce the impedance of a FCS completely different from that one used to identify the non-dimensional parameters (in terms of number of cells, electrodes surface, membrane material). Moreover, it could be possible to reduce the number of tests to be performed to fully characterize the FCS under different operating conditions, as the

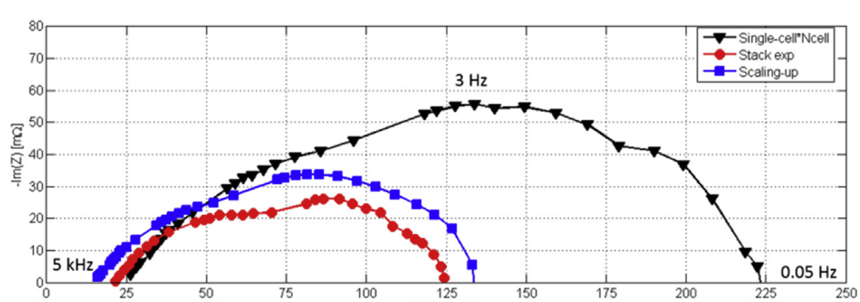

Fig. 7. Comparison of stack measured impedance (●) with: the simple multiplication of the stack last-cell impedance times the number of cells (▼) and the spectrum resulting scaling the stack last-cell impedance to obtain the full-stack impedance with the proposed methodology (■).

Table 3
Collection of the non-dimensional parameters values, as evaluated by applying the proposed Buckingham-based approach to the different cases presented above.

	G_r	G_i
From low to high current loads [29] (Fig. 3)	[0.11, 0.11, 0.11, …, 0.30, 0.34, 0.39, …, 1.01, 1.02, 1.00]	[0.01, 0.01, 0.01, …, 0.35, 0.36, 0.35, …, 0.03, 0.02, 0.01]
From low to high current loads [30] (Fig. 4)	[0.80, 0.85, 0.89, …, 2.62, 3.01, 3.5, …, 5.93, 5.91, 5.89]	[0.07, 0.17, 0.27, …, 2.17, 2.21, 2.18, …, 0.10, 0.08, 0.02]
From middle-cell to whole stack [31] (Fig. 6)	[0.08, 0.08, 0.09, …, 0.25, 0.28, 0.32, …, 0.54, 0.55, 0.55]	[0.01, 0.02, 0.04, …, 0.09, 0.10, 0.11, …, 0.06, 0.03, 0.01]
From last-cell to whole stack [31] (Fig. 7)	[0.12, 0.12, 0.13, …, 0.32, 0.35, 0.39, …, 0.99, 1.00, 0.98]	[0.01, 0.02, 0.02, …, 0.18, 0.18, 0.20, …, 0.12, 0.04, 0.02]

proposed approach allows accurately reproducing real impedance curves acquired in operating conditions falling out of the domain considered in the model development phase. Regarding the latter aspect, moving from black-box to a more physical modelling of the charge transfer resistance dependence on main operating variables (i.e. temperature and current) is expected to further strengthen the genericity features of the proposed scaling-up method.

The proposed approach can be used with several purposes such as design, diagnostics, prognostics, state of health management and on-board control, as it allows obtaining PEMFC impedance in different operating conditions with good precision and low computational effort.

Acknowledgements

The research leading to these results has received funding from the University of Salerno, by the European Community's Seventh Framework Programme (FP7/2007-2013) for the Fuel Cells and Hydrogen Joint Technology Initiative under grant agreement No. 256673 (project D-CODE – DC/DC converter-based diagnostics for PEMFC systems) and from the Fuel Cells and Hydrogen 2 Joint Undertaking under grant agreement No 671486 (project HEALTH-CODE - Real operation pem fuel cells HEALTH-state monitoring and diagnosis based on dc-dc COnverter embeddeD Eis). This Joint Undertaking receives support from the European Union's Horizon 2020 research and innovation programme and Italy, Denmark, Germany, France.

Nomenclature

AC	Alternate Current
BP	Bipolar Plates
CFD	Computational Fluid Dynamics
CL	Catalyst Layer
CWT	Continuous Wavelet Transform
DOE	Department of Energy
DWT	Discrete Wavelet Transform
ECM	Equivalent Circuit Modelling
EIS	Electrochemical Impedance Spectroscopy
FCS	Fuel Cells System
FOM	Fractional Order Modelling
FDI	Faults Detection and Isolation
GDL	Gas Diffusion Layer
PEMFC	Proton Exchange Membrane Fuel Cell

Symbols

A	electrodes area [cm^2]
C	capacitance [F]
ECSA	Electrochemical Surface Area [cm^2]
G	1st non-dimensional parameter (Z/R_{eq})
G_i	imaginary part of G ($Im(Z)/R_{eq}$)
G_r	real part of G ($Re(Z)/R_{eq}$)
I	Current [A]
I	current density [A/cm^2]
K	2nd non-dimensional parameter ($C \cdot \omega \cdot R_{eq}$)
K_m	parameter related to the membrane thickness
L	Length [m]
l_m	membrane thickness [cm]
M	Mass [kg]
N	number of variables involved
n_p	number of experimental points
N_{cell}	Number of stack cells
P	number of non-dimensional parameters
P_{sat}	saturation pressure [bar]
P_w	vapour water partial pressure [bar]
Q_i	involved physical variables
R^2	correlation coefficient
R_{ct}	Charge-transfer resistance [Ω]
R_{eq}	Equivalent resistance [Ω]
RH	Relative Humidity [/]
R_m	Membrane resistance [Ω]
T	Time [s]
T_S	stack mean temperature
v	number of physical dimensions
Z	total impedance [Ω]

Greek symbols

λ_m	membrane humidity [/]
π_i	non-dimensional parameters
σ_{30}	membrane conductivity at 30 °C [S/cm]
σ_m	membrane conductivity [S/cm]
ω	frequency [Hz]

References

[1] J. Larminie, A. Dicks, Fuel Cell Systems Explained, West Sussex, Wiley, 2003.
[2] DOE Hydrogen and Fuel Cells Program, FY, 2015 (Annual Progress report).
[3] Fuel Cells and Hydrogen 2 Joint Undertaking, Annual Work Plan, 2015.
[4] Cooper, M. Smith, Electrical test methods for on-line fuel cell ohmic resistance measurement, J. Power Sources 160 (2006) 1088–1095.
[5] Y. Tang, J. Zhang, C. Song, H. Liu, J. Zhang, H. Wang, et al., Temperature dependent performance and in situ AC impedance of high-temperature PEM fuel cells using the Nafion-112 membrane, J. Electrochem Soc. 153 (11) (2006). A 2036–43.
[6] X.Z. Yuan, C. Song, H. Wang, J. Zhang, Electrochemical Impedance Spectroscopy in PEM Fuel Cells, Springer, 2010.
[7] R. Petrone, Z. Zheng, D. Hissel, M.C. Péra, C. Pianese, M. Sorrentino, M. Becherif, N. Yousfi-Steiner, A review on model-based diagnosis methodologies for PEMFCs, Int. J. Hydrogen Energy 38 (2013) 7077–7091.
[8] Wagner N., Bauder A., Friedrich K.A., Diagnostics of PEM fuel cells, 2nd International Workshop on Degradation issues in Fuel Cells, Thessaloniki, Greece.
[9] X.Z. Yuan, J.C. Sun, H. Wang, J. Zhang, AC impedance diagnosis of a 500W PEM fuel cell stack: part II: individual cell impedance, J. Power Sources 161 (2) (2006) 929–937.
[10] M. Usman Iftikhar, D. Riu, F. Druart, S. Rosini, Y. Bultel, N. Retière, Dynamic modeling of proton exchange membrane fuel cell using non-integer derivatives, J. Power Sources, Elsevier 160 (2006) 1170–1182.
[11] C. Brunetto, A. Moschetto, G. Tina, PEM fuel cell testing by electrochemical impedance spectroscopy, Electr. Power Syst. Res. 79 (2009) 17–26.
[12] C. Xie, S. Quan, Drawing impedance spectroscopy for fuel cell by EIS, Procedia Environ. Sci. 11 (2011) 589–596.
[13] A. Narjiss, D. Depernet, D. Candusso, F. Gustin, D. Hissel, Online diagnosis of PEM fuel cell, in: 13th Power Electronics and Motion Control Conference (EPE-PEMC), IEEE, 2008, pp. 734–739.
[14] A.A. Kulikovsky, Analytical physics–based impedance of the cathode catalyst layer in a PEM fuel cell at typical working currents, Electrochim. Acta 225 (2017) 559–565.
[15] A.A. Kulikovsky, A simple physics-based equation for low-current impedance of a PEM fuel cell cathode, Electrochim. Acta 196 (2016) 231–235.

[16] A.A. Kulikovsky, PEM fuel cell impedance at open circuit, J. Electrochem. Soc. 163 (5) (2016) F319–F326.
[17] S. Cruz-Manzo, C. Perezmitre-Cruz, P. Greenwood, R. Chen, An impedance model for analysis of EIS of polymer electrolyte fuel cells under platinum oxidation and hydrogen peroxide formation in the cathode, J. Electroanal. Chem. 771 (2016) 94–105.
[18] S.M.R. Niya, R.K. Phillips, M. Hoorfar, Process modeling of the impedance characteristics of proton exchange membrane fuel cells, Electrochim. Acta 11 (2016) 594–605.
[19] B.P. Setzler, T.F. Fuller, A physics-based impedance model of proton exchange membrane fuel cells exhibiting low-frequency inductive loops, J. Electrochem. Soc. 162 (6) (2015) F519–F530.
[20] S. Chevalier, B. Auvity, J.C. Olivier, C. Josset, D. Trichet, M. Machmoum, Detection of cells state-of-health in PEM fuel cell stack using EIS measurements coupled with multiphysics modeling, Fuel Cells 14 (3) (2014) 416–429.
[21] S. Chevalier, D. Trichet, B. Auvity, J.C. Olivier, C. Josset, M. Machmoum, Multiphysics DC and AC models of a PEMFC for the detection of degraded cell parameters, Int. J. Hydrogen Energy 38 (2013) 11609–11618.
[22] E. Pahon, N. Yousfi Steiner, S. Jemei, D. Hissel, P. Moçoteguy, A signal-based method for fast PEMFC diagnosis, Appl. Energy 165 (2016) 748–758.
[23] A. Esposito, L. Russo, C. Kändler, C. Pianese, B. Ludwig, N. Yousfi Steiner, High fuel utilization in solid oxide fuel cells: experimental characterization and data analysis with continuous wavelet Transform, J. Power Sources 317 (2016) 159–168.
[24] Petrone R., Pianese C., Polverino P., Sorrentino M., International Patent Application no. PCT/IB2015/058258 claiming the priority of the Italian Patent Application no. RM2014A000641, entitled “Method For Monitoring And Diagnosing Electrochemical Devices Based On Automatic Electrochemical Impedance Identification”, 2014.
[25] E. Buckingham, Nature 96 (1915) 396.
[26] M. Sorrentino, F. Mauramati, I. Arsie, A. Cricchio, C. Pianese, W. Nesci, Application of Willans Line Method for Internal Combustion Engines Scalability towards the Design and Optimization of Eco-innovation Solutions, 2015, http://dx.doi.org/10.4271/2015-24-2397. SAE Technical Paper 2015-24-2397.
[27] M. Sorrentino, C. Pianese, M. Maiorino, An integrated mathematical tool aimed at developing highly performing and cost-effective fuel cell hybrid vehicles, J. Power Sources 221 (2013) 308–317.
[28] M. Sorrentino, C. Pianese, M. Cilento, A specification independent control strategy for simultaneous optimization of fuel cell hybrid vehicles design and energy management, in: 8th IFAC International Symposium on Advances in Automotive Control. June 19-23, 2016, Kolmården Wildlife Resort, Norrköping, Sweden, 2016.
[29] D-CODE project, Final Report, Project Coordinator: C. Pianese, 2014 website, http://www.d-code-jti.eu.
[30] S. Asghari, A. Mokmeli, M. Samavati, Study of PEM fuel cell performance by electrochemical impedance spectroscopy, Int. J. Hydrogen Energy 35 (17) (2010) 9283–9290.
[31] S. Wasterlain, D. Candusso, F. Harel, D. Hissel, X. François, Development of new test instruments and protocols for the diagnostic of fuel cell stacks, J. Power Sources, Elsevier 196 (12) (2011) 5325–5333.
[32] G.W. Hart, Multidimensional Analysis: Algebras and Systems for Science and Engineering, Springer-Verlag, 1995.
[33] S.J. Kline, Similitude and Approximation Theory, Springer-Verlag, 1986.
[34] I. Souilem, C.A. Serra, R. Muller, Y. Holl, M. Bouquey, Dimensional Analysis of a Novel Low-pressure Device for the Production of Size-tunable Nano-emulsions, vol. 61, American Institute of Chemical Engineers, 2015, pp. 23–30. N. 1.
[35] V.S. Protsenko, F.I. Danilov, Application of dimensional analysis and similarity theory for simulation of electrode kinetics described by the Marcus–Hush–Chidsey formalism, J. Electroanal. Chem. 669 (2012) 50–54.
[36] A.A. Sonin, The Physical Basis of Dimensional Analysis, second ed., Department of Mechanical Engineering MIT, 2001. Cambridge, MA 02139.
[37] T. Reshetenko, A. Kulikovsky, PEM fuel cell characterization by means of the physical model for impedance spectra, J. Electrochem. Soc. 162 (7) (2015) F627–F633.
[38] C. Wang, M.H. Nehrir, S.R. Shaw, Dynamic models and model validation for PEM fuel cells using electrical circuits, IEEE Trans. Energy Convers. 20 (2) (2005).
[39] T.E. Springer, T.A. Zawodzinski, S. Gottesfeld, Polymer electrolyte fuel cell model, J. Electrochem. Soc. 138 (8) (1991) 2334–2342.
[40] R.F. Mann, J.C. Amphlett, M.A.I. Hooper, H.M. Jensen, B.A. Peppley, P.R. Roberge, Development and application of a generalised steady-state electrochemical model for a PEM fuel cell, J. Power Sources 86 (2000) 173–180.
[41] J. Kawamura, N. Kuwata, K. Hattori, J. Mizusaki, Ionic Transport in Nano Heterogeneous Structured Materials, Reports of the Institute of Fluid Science, vol. 19, 2007, pp. 67–72.
[42] R. Petrone, Electrochemical Impedance Spectroscopy for the On-board Diagnosis of PEMFC via On-line Identification of Equivalent Circuit Model Parameters, PhD Thesis in Mechanical Engineering, XII Cycle, University of Salerno, Department of Industrial Engineering, 2011 – 2013.
[43] J. Wang, Barriers of scaling-up fuel cells: cost, durability and reliability, Energy 80 (2015) 509–521.
[44] J. Wang, Theory and practice of flow field designs for fuel cell scaling-up: a critical review, Appl. Energy 157 (2015) 640–663.
[45] K. Palaniswamy, M. Marappan, V.R. Jothi, Influence of porous carbon inserts on scaling up studies for performance enhancement on PEMFC, Int. J. Hydrogen Energy 41 (2016) 2867–2874.
[46] C. Bonnet, S. Didierjean, N. Guileet, S. Besse, T. Colinart, P. Carré, Design of an 80kWe PEM fuel cell system: scale up effect investigation, J. Power Sources 182 (2008) 441–448.
[47] A.S. Rao, Problem of scale-up in electrochemical systems, J. Appl. Electrochem. 4 (1974) 87–89.
[48] A.H. Sulaymon, A.H. Abbar, in: Kleperis, Linkov (Eds.), Scale-up of Electrochemical Reactors, Chapter 9 of Electrolysis, 2012.